Journal of Applied Surfaces and Interfaces 4 (1-3) (2018) 9-16

Journal homepage: http://revues.imist.ma/?journal=jasi

ISSN: 2550-4800

https://doi.org/10.48442/IMIST.PRSM/jasi-v4i1-3.12153

JASI JOURNAL OF APPLIED SURFACES AND INTERFACES

Synthesis of Ba doped ZnO-Al_2O_3 nanocomposite from layered double hydroxide structure and their photocatalytic activity for the degradation of caffeine

Alaâeddine Elhalil [1,], Mohamed Abdennouri [1], M'hamed Sadiq [1], Yassine Kadmi [2], Lidia Favier [3], Noureddine Barka [1].*

[1] *Laboratoire LS3M, FP Khouribga, Université Sultan Moulay Slimane, B.P. 145, 25000 Khouribga, Morocco.*
[2] *Université de Lille, LASIR; UMR CNRS 8516, Villeneuve d'Ascq, France.*
[3] *Ecole Nationale Supérieure de Chimie de Rennes, CNRS, UMR 6226, 11 Allée de Beaulieu, CS 50837, 35708 Rennes Cedex 7, France.*

Received 24 April 2018; Revised 15 October 2018; Accepted 27 October 2018.

Abstract : *In this research, $BaCO_3$/ZnO-Al_2O_3 nanocomposite photocatalyst at different amount of Ba (1, 3 and 5 wt%) was prepared from Zn-Al-CO_3 layered double hydroxides precursors using ceramic process. A range of physicochemical techniques including X-ray diffraction (XRD), Fourier transform infrared spectroscopy (FTIR) and scanning electron microscope (SEM) with energy dispersive X-ray analysis (EDX), were employed to characterize the as-prepared catalysts. The photocatalytic activity of the catalysts was evaluated for the photocatalytic degradation of caffeine as a model of pharmaceutical pollutant in aqueous solutions under UV irradiation. Detailed photocatalytic experiments based on the effects of dopant amount, irradiation time, catalyst dose, initial pH and reuse were performed and presented in this study. The enhancement of photocatalytic activity was strongly dependent on the Ba amount and adsorption process. The 1%Ba/ZnO-Al_2O_3 sample with high adsorption capacity showed the highest photocatalytic activity with a degradation efficiency of 98.2% after 70 min of irradiation. It showed a significantly higher rate of degradation compared to undoped, pure ZnO and standard Degussa P-25 titanium dioxide. The photocatalyst showed high stability after three regeneration cycles.*

Keywords: *Ba/ZnO-Al_2O_3; Mixed metal oxides photocatalyst; Photocatalytic property; Caffeine degradation, UV irradiation.*

1. Introduction

Pharmaceutical and personal care products have received increased attention as aquatic contaminants due to the extensive use of antibiotics, mental drags and hormone drugs from synthetic or natural sources [1]. Caffeine ($C_8H_{10}N_4O_2$) is the most consumed psychoactive drugs worldwide [2]. It is a naturally occurring alkaloid present in many plant species including coffee seeds, citrus fruits, tea leaves, cocoa beans, yaupon and guarana [3]. As a dietary component widely found in common food and beverages, the caffeine content of coffee and tea is especially high. Due to its stimulatory nature, caffeine is also used as a stimulant or adjuvant in psychoactive medicine [4].

Because of its wide use in food and pharmaceutical industries, caffeine enters the environment via liquid effluents and solid waste from processing facilities and domestic waste. The harmful effects of caffeine when discharged into the environment have been well documented. However, it can cause adverse mutation effects when excessively consumed [5], such as mutagenic effects in DNA repair and cyclic AMP phosphodiesterase activity [6-8]. Furthermore, it can be a cause of cancer, heart diseases and complications in pregnant women and aging.

The presence of caffeine in soil can also affect soil fertility as it inhibits seed germination and growth of seedlings [9]. Because it is so frequently observed in the aquatic environment, including wastewater, surface water and ground water [10-12], caffeine can be an anthropogenic marker for contaminated source water [13] and have been listed as an emerging organic contaminant [14-16]. It is therefore reasonable to proclaim that caffeine degradation is an important matter for health as well as for the general environment.

Advanced oxidation processes (AOPs) are generally recognized as the most effective methods for the degradation of hazardous, refractory and non-biodegradable organic pollutants, because of the generation of reactive hydroxyl radicals ($^{\bullet}OH$). The typical AOPs involve in catalytic ozonation [17], Heterogeneous photocatalysis [18,19] and Fenton process [20]. Heterogeneous photocatalysis, one of the AOPs, is an effective process for the degradation of persistent pollutants. One of the main reasons is the ability of the process to achieve the degradation and mineralization of many organic pollutants at normal conditions of temperature and pressure, with a fairly clean technology [21-24].

* *Corresponding author: E-mail: elhalil.alaaeddine@gmail.com (Alaâeddine Elhalil)*

Up to now, many different of oxides semi-conductors have been developed, such as TiO_2 [25], WO_3 [26], ZnO [27], ZnS [28], Bi_2O_3 [29], CdS [30], etc. Among theme, ZnO a multifunctional semiconductor photocatlyst, has been widely investigated due to its thermal conductivity, chemical stability and good UV absorption properties [31]. Nevertheless, it is noteworthy that ZnO has some shortcomings, including fast recombination rate of photogenerated electron /hole pairs and a low quantum yield of the photocatalytic reactions in aqueous solution, which obstruct its full scale application as a photocatalyst [32,33]. Therefore, several efforts have been made to reduce the e-/h+ recombination rate of ZnO by modification or by doping with several elements such as transition metals [34], non-metals [35] and noble metals [36], or by alkaline earth metals [37].

Various techniques have been used to elaborate ZnO oxide, such as sol-gel technique [38], hydrothermal synthesis method [39], chemical vapor deposition [40], photo-chemical reduction processes [41], co-precipitation method [42], spray-pyrolysis method [43], ultrasound-assisted method [44], and microwave-assisted thermal decomposition [45]. By using layered double hydroxides (LDH) as precursor for the preparation of ZnO it is possible to obtain a fine dispersion of active components on the surface of semiconductor, and as a consequence the formation of an intimate contact at atomic level between the generated semiconductor phases. Moreover, Al in the structure has more advantages over ZnO photocatalyst owing to its high photocatalytic activity, morphology, particle size and good stability [46-48].

In this study, $BaCO_3$/ZnO-Al_2O_3 heterostructure photocatalyst with different content of Ba (1, 3 and 5 wt%) was prepared from Zn-Al-CO_3 layered double hydroxides precursors using ceramic process. The photocatalysts were characterized by several physico-chemical techniques (XRD, FTIR and SEM/EDX). The photocatalytic activity of prepared photocatalysts was evaluated for the degradation of caffeine as model of pharmaceutical pollutant under UV irradiation. The effect of Ba doping concentration on the photocatalytic activity was investigated in detail.

2. Experimental

2.1. Reagents

The starting chemicals; zinc nitrate $Zn(NO_3)_2.6H_2O$ (≥ 99%), aluminum nitrate $Al(NO_3)_3.9H_2O$ (≥ 98%), barium nitrate $Ba(NO_3)_2$ (≥ 99%), sodium carbonate Na_2CO_3 (≥ 99%), sodium hydroxide NaOH (≥ 99%), hydrochloric acid HCl, (≥ 37%) and standard Degussa P-25 titanium dioxide (≥ 99,5%) have been acquired from Sigma-Aldrich (Germany). Degussa P-25 titanium dioxide has a specific surface area of 50±5 m^2/g and is composed of 80% anatase and 20% of rutile [49], which was used in this study as a reference photocatalyst. Caffeine ($C_8H_{10}N_4O_2$, 100%) was a product of Sigma-Aldrich (China). Nitric acid HNO_3, (≥ 65%) extra pure was purchased from Scharlau chemie (Spain) and Sodium chloride NaCl (≥ 99.5%) from Fluka (Germany). All the used chemicals were of analytical grade and were used without further purification. Bidistilled water was used as the solvent throughout this study.

2.2. Catalysts preparation

2.2.1. Synthesis of LDH precursor and ZnO-Al_2O_3 photocatalyst

Zn-Al-CO_3 LDH precursor with Zn/Al molar ratio of 3 was synthesized by co-precipitation method. $Zn(NO_3)_2{\cdot}6H_2O$ and $Al(NO_3)_3{\cdot}9H_2O$ with the total concentration of metal ions fixed at 2 mol/L were dissolved in 200 mL of bidistilled water [50]. The Na_2CO_3 (100 mL, 1 mol/L) solution as a source of carbonate and the metal nitrates solutions were added drop-wise in a backer containing 50 mL of bidistilled water, the pH of the solution was maintained at 8.5±0.2 by adding NaOH (2 mol/L) as precipitant agent, under vigorous magnetic stirring for 4 h. The formed gel was then transferred into an autoclave and hydrothermally treated at 75 °C (16 h). The obtained white precipitates were filtered, washed several times with bidistilled water (until pH=7) to remove any ions possibly remaining in the final materials, and then dried at 100 °C for 24 h. The resulting product (Zn-Al-CO_3) was ground into fine powder and stored in sample bottles for further use. The mixed metal oxides photocatalyst was prepared by calcination of LDH precursor at 500 °C for 6 h in muffle furnace. The sample was labeled as ZnO-Al_2O_3.

2.2.2. Solid state impregnation

Desired amount of LDH precursor and Ba(NO3)2 were manually ground in an agate mortar for 30 min. After that the homogeneously mixed powder was transferred into a crucible and calcined in air at 500 °C for 6 h in muffle furnace. The entire process is free of solvent. The obtained samples were denoted as x%Ba/ZnO-Al_2O_3, where x% represent the weight percentage of Ba in the mixture (1, 3, and 5 wt%).

2.2.3. Synthesis of pure ZnO

For comparison, pure ZnO oxide powder was prepared using precipitation method. Firstly, $Zn(NO_3)_2{\cdot}6H_2O$ was dissolved in distilled water under stirring to form a clear solution. Subsequently, the pH of solution was adjusted to 8.5 with NaOH (2 mol/L) added dropwise. After stirring for 4h, the mixture solution was transferred to a 500 mL flask and heated at 75 °C for 16 h. After that, the precipitate is filtered, washed several times with deionized water and dried at 100 °C for 24 h. Finally, the product was calcined at 500 °C for 6 h to obtain the pure ZnO oxide.

2.3. Characterization

The XRD measurements were performed at room temperature on a D2 PHASER diffractometer, with the

Bragg–Brentano geometry, using CuKα target (λ=0.15406 nm) operated at 30 KV and 10 mA. The XRD scans were recorded in the 2θ range 10–80° with step size 0.01° (0.5s/step). Fourier transform infrared (FTIR) spectra in KBr pellets were collected on a Perkin Elmer (FTIR-2000) spectrophotometer, in the range of 4000-400 cm^{-1}. The external surface of sample was analyzed by scanning electron microscopy coupled to the energy dispersive X-ray spectroscopy (SEM/EDX) by a FEI Quanta 200 model, using an accelerating voltage of 20 kV. The point of zero charge (pH_{PZC}) was determined by the pH drift method according to the method proposed by Noh and Schwarz [51]. The pH of NaCl aqueous solution (50 mL at 0.01 mol/L) was adjusted to successive initial values in the range of 2-12 by addition of HNO_3 and/or NaOH. Moreover, 0.05 g of each biosorbent was added in the solution and stirred for 6 h. The final pH was measured and plotted vs. the initial pH. The pH_{PZC} was determined at the value for which $pH_{final} = pH_{initial}$.

2.4. Adsorption/photocatalytic measurements

The photocatalytic performance of the photocatalysts was studied by degradation of caffeine in water solution. Experiments were done using 0.3 g/L of each photocatalyst with an initial caffeine concentration equal to 20 mg/L. The reaction was carried out in a cylindrical Pyrex photoreactor with a capacity of 2 L and was initiated by a UV mercury lamp (400 W) placed in the center of the reactor. The temperature was maintained at 25±2 °C by connecting the reactor to circulating water for preventing the lamp from overheating. Before irradiation, the mixtures were vigorously stirred for 60 min under dark to establish an adsorption/desorption equilibrium on the surface of catalysts. During irradiation, the mixture was stirred at a constant rate under continuous O_2 flow. At given time intervals, 3 mL aliquots were sampled and filtered to remove the solid particles. The filtrates were analyzed using a double-beam scanning spectrophotometer (Shimadzu spectrophotometer, model biochrom) at maximum wavelength of 273 nm, characteristic to caffeine. The percentage of degradation was calculated by C/C_0, where C is the concentration of remaining caffeine solution at each irradiated time interval, while C_0 is the initial concentration.

3. Results and discussion

3.1. Catalysts characterization

3.1.1. X-ray diffraction (XRD) study

XRD patterns of LDH precursor before and after calcination, pure ZnO and Ba-doped ZnO-Al_2O_3 are shown in Fig.1. The figure exhibits the characteristic reflections of the LDH structure with planes (003), (006), (012), (015), (018), (110) and (113). No impurities from any residual $Zn(OH)_2$ or $Al(OH)_3$ were observed. The XRD pattern of the synthetic LDH was identical to that of natural hydrotalcite, JCPDS card 22-700 [52]. Remarkable changes are observed after calcination at 500 °C. The lamellar structure collapsed and new peaks corresponding to ZnO oxide appear. The characteristic XRD peaks of ZnO oxide started to appear indicated by the peaks at 2θ = 31.8°, 34.5°, 36.3°, 47.6°, 56.6°, 62.9°, 66.4°, 68° and 69.1°. These peaks correspond to the reflections from (100), (002), (101), (102), (110), (103), (200), (112) and (201) planes, respectively, this is also confirmed by the JCPDS data (Card No. 36- 1451) [53].

Total dehydroxylation was observed at 500 °C and resulted in the transformation of LDH structure to corresponding metal oxides ZnO and Al_2O_3. There is no detection of signals corresponding to Al_2O_3 phase, implying that Al_2O_3 is amorphous [54]. The characteristic diffraction peaks of synthesized pure ZnO match well with the standard card of ZnO oxide [53].

For Ba-doped ZnO-Al_2O_3 samples, additional peaks at 23.89°, 24.31°, 27.72°, 41.99°, 42.97°, 44.17°, 44.94° and 46.77° were observed. These peaks can be assigned to (111), (021), (002), (221), (041), (202), (132) and (113) reflections of pure orthorhombic $BaCO_3$ single phase (witherite), this is also confirmed by the JCPDS data (Card No. 05-0378) [55]. The intensity of Ag nanoparticles was much sharper and increases with increasing Ag content. No peaks from other phases were detected, indicating high purity of the products.

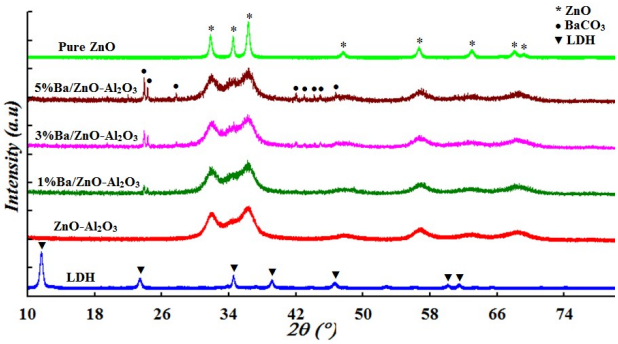

Fig.1. *XRD patterns of fresh LDH precursor, pure ZnO, undoped and Ba doped ZnO-Al_2O_3.*

3.1.2. Fourier transform infrared (FTIR) spectra

Fig.2 represents the FTIR spectra of fresh LDH precursor, undoped and Ba doped LDH calcined at 500 °C. The spectrum of the fresh LDH precursor shows a broad band between 3600 and 3200 cm^{-1}, which is attributed to the stretching vibration of the OH groups of physically adsorbed and interlamellar water molecules. The band at 1617 cm^{-1} was due the O–H bending vibration of the interlayer water molecules [56]. The band at 1364 cm^{-1} is assigned to the stretching vibration of the CO_3^{2-} groups in the LDH interlayer [57]. This band rapidly disappears after calcination, which is attributed to the thermal decomposition of carbonate ions. After doping, the typical bands of CO_3^{2-} (1364 cm^{-1}) still exist. This band was due to the formation of $BaCO_3$ phase. The XRD analysis confirms their formation.

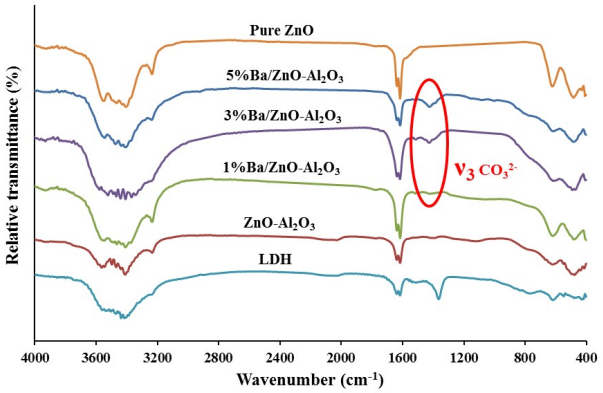

Fig.2. *FTIR spectra of fresh LDH precursor, pure ZnO, undoped and Ba doped ZnO-Al_2O_3.*

3.1.3. SEM/EDX

The morphology and microstructure of the ZnO-Al_2O_3 and 1%Ba/ZnO-Al_2O_3 photocatalysts were investigated by SEM. As shown in Fig.3(a,c), surface morphology of these samples is more different from each other. It is clearly seen that photocatalysts has a heterogeneous surface with observable porosity. For 1%Ba/ZnO-Al_2O_3, $BaCO_3$ particles were homogeneously and highly dispersed on the surface of ZnO-Al_2O_3 material. Energy dispersive X-ray spectrum (EDX) of undoped and Ba doped composite is shown in Fig.3(b,d). The results confirm the presence of Zn, Al and O in the undoped sample. For 1%Ba/ZnO-Al_2O_3 composite, the spectrum shows peaks corresponding to Ba and C along with the other constituent elements (Zn, Al and O).

3.2. Photocatalytic study

3.2.1. Effect of Ba doping

The adsorption/photocatalytic performance of undoped and Ba doped ZnO-Al_2O_3 nanocomposite in comparaison with pure ZnO and P-25 titanium dioxide in the same experimental conditions for caffeine degradation under UV light irradiation is presented in Fig.4. In the same operating conditions for the photocatalytic degradation, the photolytic degradation (direct photolysis) without photocatalysts was studied. It could be seen that the degradation of caffeine is very low in the absence of photocatalysts under UV light irradiation. In the adsorption phase, pure ZnO and P-25 titanium dioxide have hardly any adsorption of caffeine after stirred for 60 min. The adsorption efficiencies of caffeine on ZnO-Al_2O_3, 1%Ba/ZnO-Al_2O_3, 3%Ba/ZnO-Al_2O_3 and 5%Ba/ZnO-Al_2O_3 are 7%, 10.16%, 5.47 and 2.66%, respectively. Clearly, 1%Ba/ZnO-Al_2O_3 exhibits much higher adsorptive ability than other catalysts. While the adsorption process decreases in the presence of 3%Ba/ZnO-Al_2O_3 and 5%Ba/ZnO-Al_2O_3 catalysts respectively.

As it can be observed, there was an important decrease of the caffeine concentration during the irradiation in the presence of all the prepared photocatalysts in comparison to the photolysis. The pure ZnO exhibits moderate photocatalytic activity with the degradation percentage of 60.8% after 70 min of irradiation, while the ZnO-Al_2O_3 photocatalyst synthesized from layered double hydroxides precursor enhances greatly the photcatalytic activitie (89.18%, 70 min). The photocatalytic activity of Ba doped ZnO-Al_2O_3 catalysts increased with the increase of Ba content until 1 % and then decreased when Ba content was higher than 3%. It was evident that the 1%Ba/ZnO-Al_2O_3 nanocomposites showed the highest photocatalytic degradation, as this sample degraded the caffeine by about 98.2% within 70 min of irradiation. The Ba doped ZnO-Al_2O_3 photocatalysts shows an improved activity, higher than the commercial P-25 photocatalyst.

The adsorption ability is very important during the photocatalytic process, very high adsorptive efficiency will accelerate the degradation process. This behavior was confirmed by the great correlation between adsorbed quantity and photocatalytic degradation of caffeine on 1%Ba/ZnO-Al_2O_3, 3%Ba/ZnO-Al_2O_3 and 5%Ba/ZnO-Al_2O_3 photocatalysts, as shown in Fig.5. These results suggested that, the synergistic effect between $BaCO_3$ and ZnO-Al_2O_3 material and adsorption process were benefit in the enhancement of the photocatalytic degradation of caffeine.

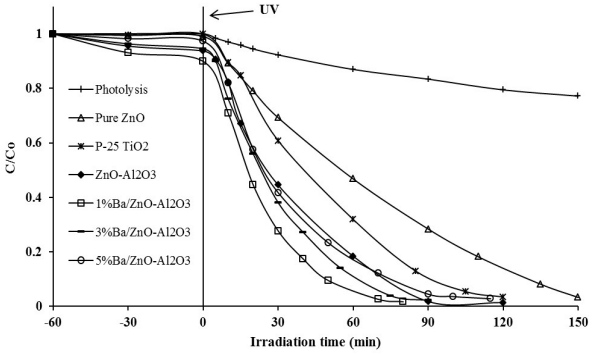

Fig.4. *Photocatalytic degradation of caffeine in the presence of undoped and Ba doped ZnO-Al_2O_3 compared to pure ZnO and standard Degussa P-25 TiO2 (Caffeine concentration: 20 mg/L; photocatalyst dosage: 0.3 g/L; pH of the natural solution (~7.5)).*

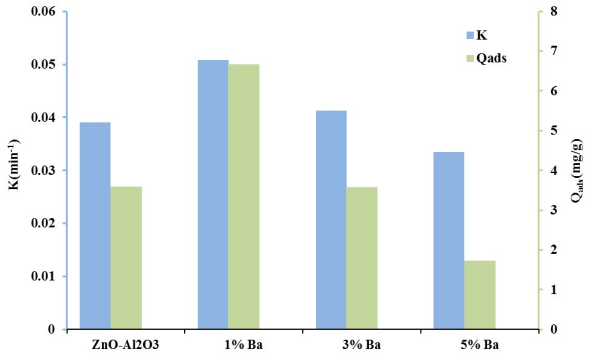

Fig.5. *Correlation between adsorbed quantity and photocatalytic degradation rate of caffeine.*

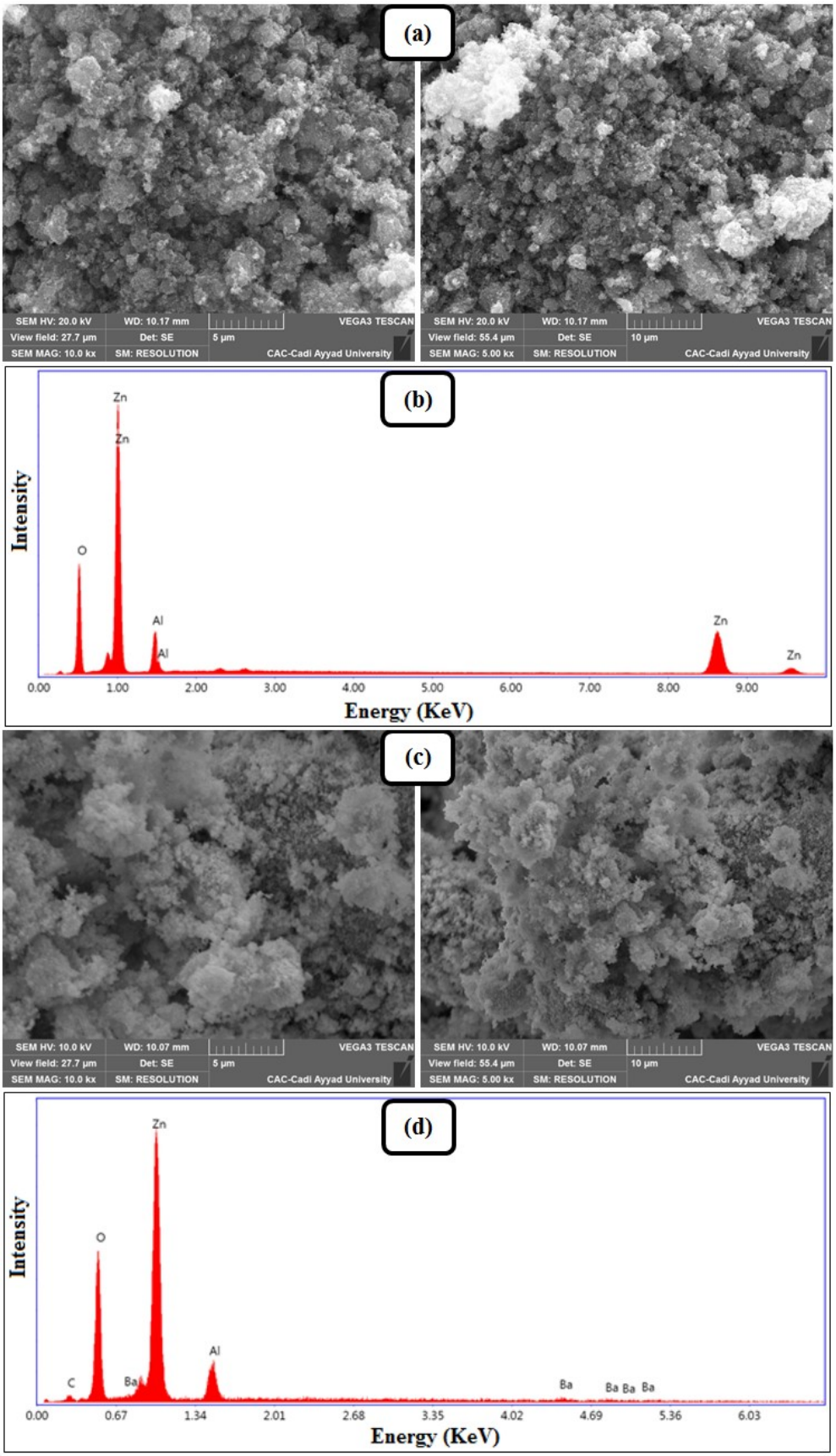

Fig.3. *SEM-EDX images of undoped (a, b) and 1% Ba doped composite (c, d).*

3.2.2. Effect of photocatalyst dose

In order to avoid excess catalyst and ensure total absorption of efficient photons, series of experiments was carried out to assess the optimum catalyst loading by varying the amount of the best photocatalyst (1%Ba/ZnO-Al_2O_3) from 0.1 to 1.5 g/L. Experiments were done with 20 mg/L caffeine aqueous solution at initial solution pH of 7.5. After 70 min of UV irradiation, the photocatalytic degradation efficiency was evaluated. Results given in Fig.6 showed that the increase in photocatalyst dose from 0.1 to 0.3 g/L resulted in an increase in the photocatalytic degradation efficiency from 64.14 to 98.2%. Beyond this dose, a slight decrease with the rise of the dose was observed. This can be explained by the fact that excess photocatalyst dose resulted in an unfavorable light scattering and a reduction of light penetration into the solution [58]. From a practical viewpoint, the optimum dosage of 0.3 g/L was chosen in furthers experiments.

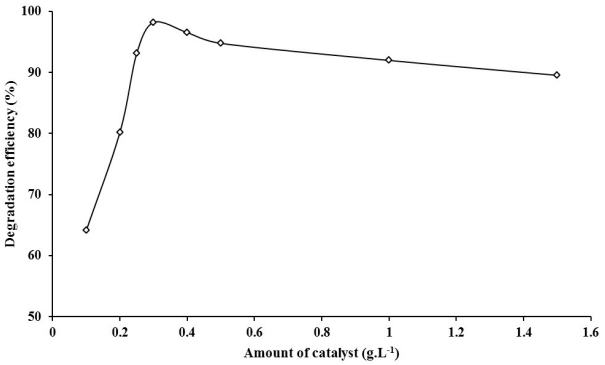

Fig.6. *Effect of catalyst dose on the photocatalytic degradation of caffeine (Caffeine concentration: 20 mg/L; initial solution pH: ~7.5).*

3.2.3. Effect of initial solution pH

The effect of solution pH on photocatalytic oxidation of caffeine in presence of 1%Ba/ZnO-Al_2O_3 was studied at pH of 3.5, 7.5 and 9.5. Fig.7 shows that solution pH affected significantly the percentage degradation of caffeine. The photocatalytic activity was enhanced at pH of 9.5 and was dramatically decreased at pH of 3.5. Generally, solution pH affects at the same time the surface charge of the photocatalyst and the ionization of caffeine molecules in solution. The pH_{pzc} of 1%Ba/ZnO-Al_2O_3 catalyst was found to be 9.23. Therefore, at pH>9.23 the surface acquire negative charge, favoring the adsorption of cationic molecules. While at pH<9.23, the surface of the catalyst acquire positive charge, favoring the adsorption of anionic molecules. The pKa of caffeine molecule is 10.4 which means that the molecule is fully protonated at pH<10.4.

Since the structure of caffeine was the same in the region of studied pH, the observed behavior could be only due to the modification of the proprieties of the photocatalysts. The observed trend of the photocatalytic activity observed at pH of 9.5 could be due to the enhanced adsorption of caffeine on the photocatalyst favored at pH between 9.23 and 10.4 and more efficient formation of hydroxyl radicals. In acidic medium (pH=3.5), the decrease of the percentage degradation could be attributed to many phenomena simultaneously intervening: a) non favorable adsorption, b) the dissolution of the photocatalysts and c) the photodecomposition and dissolution of ZnO according to the following equations [59]:

Dissolution: $ZnO + 2H^+ \rightarrow Zn^{2+}_{(aq)} + H_2O$ (1)

Photodecomposition: $ZnO + 2h^+_{VB} \rightarrow Zn^{2+}_{(aq)} + O^*$ (2)

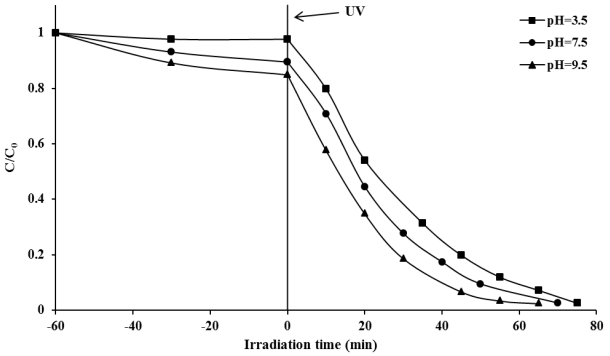

Fig.7. *Effect of initial solution pH on the photocatalytic degradation of caffeine (Caffeine concentration: 20 mg/L; photocatalyst dosage: 0.3 g/L).*

3.2.4. Efficiency of regenerated photocatalyst

Recycling of the photocatalyst is crucially important for industrial applications [60]. In order to determine the recyclability of the best catalyst (1%Ba/ZnO-Al_2O_3), we carried out a cycle of experiment under identical conditions. In each experiment, after using the nanocomposite in one cycle, it was washed with distilled water and dried at 100 °C for 24 h. As illustrated in Fig.8, the photocatalytic activity of the prepared photocatalyst still maintains a high level even after 3 times cycling.

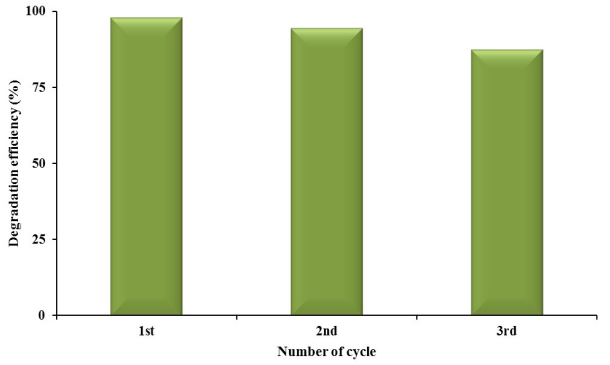

Fig.8. *Photocatalytic degradation of caffeine over three cycles of regeneration of 1%Ba/ZnO-Al_2O_3 photocatalyst (Caffeine concentration: 20 mg/L; photocatalyst dosage: 0.3 g/L; solution pH: ~7.5).*

As shown in figure, the 1%Ba/ZnO-Al_2O_3 nanocomposite reveals high photostability in these experiments, although a slight decrease of activity is observed compared to the first-run result (10.58%). This

can be attributed to residual caffeine adsorbed on surface of catalyst. The results suggest that the 1%Ba/ZnO-Al_2O_3 nanocomposite may have practical application potentials as an effective and stable photocatalyst for degradations of different pharmaceutical pollutants under UV irradiation.

4. Conclusion

$BaCO_3$/ZnO-Al_2O_3 heterostructured catalysts at various contents of Ba (1, 3 and 5 wt%) were successfully synthesized from LDH precursors by ceramic process. The synthesized photocatalysts were characterized by several physicochemical techniques including XRD, FTIR and SEM/EDX. The 1%Ba/ZnO-Al_2O_3 catalyst exhibited higher photocatalytic activity than ZnO-Al_2O_3, pure ZnO and commercial Degussa P-25 titanium dioxide catalysts for the degradation of caffeine under UV light irradiation. The excellent photocatalytic activity of 1%Ba/ZnO-Al_2O_3 was attributed to the adsorption process and interfacial heterostructure in the $BaCO_3$/ZnO-Al_2O_3 catalysts. The optimum catalyst dosage for the degradation of a 20 mg/L of caffeine solution was found to be 0.3 g/L. It was observed that the adsorption of the caffeine onto 1%Ba/ZnO-Al_2O_3 nanostructure surface is strongly dependent on the pH of the solution which plays an important role in photocatalytic degradation and the optimal pH was 9.5. The recycling tests indicated high stability in the photocatalytic performance.

References

[1] F. Bonvin, R. Rutler, N. Chevre, J. Halder, T. Kohn, Environmental Science and Technology 45 (2011) 4702–4709.

[2] R. Lovett, New Scientist (2005) 38–41.

[3] K. Manoli, G. Nakhla, M. Feng, V.K. Sharma, A.K. Ray, Chemical Engineering Journal 330 (2017) 987–994.

[4] A. Nehlig, J.L. Daval, G. Debry, Brain Research Reviews 17 (1992) 139–169.

[5] F.W. Pons, P. Muller, Mutagenesis 5 (1990) 173–177.

[6] K. Tyszczuk-Rotko, I. Beczkowska, Food Chemistry 172 (2015) 24–29.

[7] W.D.J.R. Santos, M. Santhiago, I.V.P. Yoshida, L.T. Kubota, Sensors and Actuators, B: Chemical 166–167 (2012) 739–745.

[8] J.-Y. Sun, K.-J. Huang, S.-Y. Wei, Z.-W. Wu, F.-P. Ren, Colloids and Surfaces B: Biointerfaces 84 (2011) 421–426.

[9] S. Nanjundaiah, S. Mutturi, P. Bhatt, Biochemical Engineering Journal 125 (2017) 73–80.

[10] Q. Sui, J. Huang, S.B. Deng, G. Yu, Q. Fan, Water Research 44 (2010) 417–426.

[11] R.L. Seiler, S.D. Zaugg, J.M. Thomas, D.L. Howcroft, Ground Water 37 (1999) 405–410.

[12] F. Qi, W. Chu, B.B. Xu, Chemical Engineering Journal 235 (2014) 10–18.

[13] I.J. Buerge, T. Poiger, M.D. Muller, H.R. Buser, Environmental Science & Technology, 37 (2003) 691–700.

[14] M.K. Arfanis, P. Adamou, N.G. Moustakas, T.M. Triantis, A.G. Kontos, P. Falaras, Chemical Engineering Journal 310 (2017) 525–536.

[15] O.M. Rodriguez-Narvaez, J.M. Peralta-Hernandez, A. Goonetilleke, E.R. Bandala, Chemical Engineering Journal 323 (2017) 361–380.

[16] T. Deblonde, C. Cossu-Leguille, P. Hartemann, International Journal of Hygiene and Environmental Health 214 (2011) 442–448.

[17] S. Esplugas, D.M. Bila, L.G.T. Krause, M. Dezotti, Journal of Hazardous Materials 149 (2007) 631–642.

[18] A. Elhalil, R. Elmoubarki, A. Machrouhi, M. Sadiq, M. Abdennouri, S. Qourzal, N. Barka, Journal of Environmental Chemical Engineering 5 (2017) 3719–3726.

[19] N. Barka, S. Qourzal, A. Assabbane, A. Nounah, Y. Ait-Ichou, Chemical Engineering Communications 198 (2011) 1233–1243.

[20] A. Elhalil, H. Tounsadi, R. Elmoubarki, F.Z. Mahjoubi, M. Farnane, M. Sadiq, M. Abdennouri, S. Qourzal, N. Barka, Water Resources and Industry 15 (2016) 41–48.

[21] J. Herney-Ramirez, M.A. Vicente, L.M. Madeira, Applied Catalysis B 98 (2010) 10–26.

[22] A. Kambur, G.S. Pozan, I. Boz, Applied Catalysis B 115 (2012) 149–158.

[23] C. Diaz-Uribe, W. Vallejo, W. Ramos, Applied Surface Science 319 (2014) 121–127.

[24] G. Liao, D. Zhu, J. Zheng, J. Yin, B. Lan, L. Li, Journal of the Taiwan Institute of Chemical Engineers 67 (2016) 300–305.

[25] H.L. Shen, H.H. Hu, D.Y. Liang, H.L. Meng, P.G. Li, W.H. Tang, C. Cui, Journal of Alloys and Compounds 542 (2012) 32–36.

[26] H. Zhang, J. Yang, D. Li, W. Guo, Q. Qin, L. Zhu, W. Zheng, Applied Surface Science 305 (2014) 274–280.

[27] R. Khan, M.S. Hassan, L.W. Jang, J.H. Yun, H.K. Ahn, M.S. Khil, I.H. Lee, Ceramics International 40 (2014) 14827–14831.

[28] Q. Ma, Y. Wang, J. Kong, H. Jia, Ceramics International 42 (2016) 2854–2860.

[29] D. Sánchez-Martínez, I. Juárez-Ramírez, L.M. Torres-Martínez, I. De León-Abarte, Ceramics International 42 (2016) 2013–2020.

[30] Z. Yu, B. Yin, F. Qu, X. Wu, Chemical Engineering Journal 258 (2014) 203–209.

[31] A.H.A.M. Gratzel, Chemical Reviews 95 (1995) 49–68.

[32] H. Osman, Z. Su, X. Ma, S. Liu, X. Liu, D. Abduwayit, Ceramics International 42 (2016) 10237–10241.

[33] K.M. Lee, C.W. Lai, K.S. Ngai, J.C. Juan, Water Research 88 (2016) 428–448.

[34] W. Bousslama, H. Elhouichet, M. Férid, Optik 134 (2017) 134, 88–98.

[35] P.M. Perillo, M.N. Atia, Nano-Structures & Nano-Objects 10 (2017) 125–130.

[36] C. Yu, K. Yang, W. Zhou, Q. Fan, L. Wei, J.C. Yu, Journal of Physics and Chemistry of Solids 74 (2013) 1714–1720.

[37] S. Klubnuan, P.Amornpitoksuk, S. Suwanboon, Materials Science in Semiconductor Processing 39 (2015) 515–520.

[38] B. Astinchap, R. Moradian, M.N. Tekyeh, Optik. 127 (2016) 9871–9877.

[39] B. Liu, H.C. Zeng, Journal of the American Chemical Society 125 (2003) 4430–4431.

[40] Y. Liu, M. Liu, Journal of Nanoscience and Nanotechnology 7 (2007) 4529–4533.

[41] G. Oster, M. Yamamoto, Journal of Physical Chemistry 70 (1966) 3033–3036.

[42] S. Akir, A. Barras, Y. Coffinier, M. Bououdina, R. Boukherroub, A.D. Omrani, Ceramics International 42 (2016) 10259–10265.
[43] T. Tharsika, A.S.M.A. Haseeb, S.A. Akbar, M. Thanihaichelvan, Ceramics International 41 (2015) 5205–5211.
[44] O. Carp, A. Tirsoaga, R. Ene, A. Ianculescu, R.F. Negrea, P. Chesler, G. Ionita, R. Birjega, Ultrasonics Sonochemistry 36 (2017) 326–335.
[45] F. Solis-Pomar, A. Jaramillo, J. Lopez-Villareal, C. Medina, D. Rojas, A.C. Mera, M.F. Meléndrez, E. Pérez-Tijerina, Ceramics International 42 (2016) 18045–18052.
[46] L. Duan, X. Zhao, Z. Zheng, Y. Wang, W. Geng, F. Zhang, Journal of Physics and Chemistry of Solids 76 (2015) 88–93.
[47] X. Xing, D. Deng, Y. Li, N. Chen, X. Liu, Y. Wang, Ceramics International 42 (2016) 18914–18924.
[48] X. Zhang, Y. Chen, S. Zhang, C. Qiu, Separation and Purification Technology 172 (2017) 236–241.
[49] N. Barka, I. Bakas, S. Qourzal, A. Assabbane, Y. Ait-Ichou, Oriental Journal of Chemistry 29 (3) (2013) 1055–1060.
[50] A. Elhalil, R. Elmoubarki, M. Farnane, A. Machrouhi, F.Z. Mahjoubi, M. Sadiq, S. Qourzal, N. Barka, Materials Today Communications 16 (2018) 194–203.
[51] J.S. Noh, J.A. Schwarz, Journal of Colloid and Interface Science 130 (1989) 157–164.
[52] T. Kameda, M. Saito, Y. Umetsu, Materials Transactions 47(3) (2006) 923–930.
[53] G.P. Sahoo, S. Samanta, D.K. Bhui, S. Pyne, A. Maity, A. Misra, Journal of Molecular Liquids 212 (2015) 665–670.
[54] L. Zhang, C-H. Dai, X-X. Zhang, Y-N. Liu, J-H. Yan, Transactions of Nonferrous Metals Society of China 26 (2016) 2380−2389.
[55] B. CHENG, X. YU, J. YU, X. ZHAO, Rare Metals 25 (2006) 382−388.
[56] A.A.A. Ahmed, A.T. Zainal, Z.H. Mohd, Z. Azmi, Journal of Alloys and Compounds 539 (2012) 154–160.
[57] S. Li, Z. Bai, D. Zhao, Applied Surface Science 284 (2013) 7–12.
[58] A. Elhalil, R. Elmoubarki, M. Farnane, A. Machrouhi, M. Sadiq, F.Z. Mahjoubi, S. Qourzal, N. Barka, Environmental Nanotechnology, Monitoring & Management 10 (2018) 63–72.
[59] N. Daneshvar, D. Salari, A.R. Khataee, Journal of Photochemistry and Photobiology A: Chemistry 162 (2004) 317–322.
[60] A. Elhalil, R. Elmoubarki, M. Sadiq, M. Abdennouri, Y. Kadmi, L. Favier, S. Qourzal, N. Barka, Desalination and Water Treatment 94 (2017) 254–262.